JOC The Journal of Organic Chemistry

Article

pubs.acs.org/joc

Role of the P−F Bond in Fluoride-Promoted Aqueous VX Hydrolysis: An Experimental and Theoretical Study

Daniele Marciano,[§,†] Ishay Columbus,[§,†] Shlomi Elias,[†] Michael Goldvaser,[†] Ofir Shoshanim,[‡] Nissan Ashkenazi,*[,†] and Yossi Zafrani*[,†]

[†]Department of Organic Chemistry and [‡]Department of Environmental Physics, Israel Institute for Biological Research, Ness-Ziona, 74100, Israel

Supporting Information

ABSTRACT: Following our ongoing studies on the reactivity of the fluoride ion toward organophosphorus compounds, we established that the extremely toxic and environmentally persistent chemical warfare agent VX (*O*-ethyl *S*-2-(diisopropylamino)ethyl methylphosphonothioate) is exclusively and rapidly degraded to the nontoxic product EMPA (ethyl methylphosphonic acid) even in dilute aqueous solutions of fluoride. The unique role of the P−F bond formation in the reaction mechanism was explored using both experimental and computational mechanistic studies. In most cases, the "G-analogue" (*O*-ethyl methylphosphonofluoridate, Et-G) was observed as an intermediate. Noteworthy and of practical importance is the fact that the toxic side product desethyl-VX, which is formed in substantial quantities during the slow degradation of VX in unbuffered water, is completely avoided in the presence of fluoride. A computational study on a VX-model, *O*,*S*-diethyl methylphosphonothioate (**1**), clarifies the distinctive tendency of aqueous fluoride ions to react with such organophosphorus compounds. The facility of the degradation process even in dilute fluoride solutions is due to the increased reactivity of fluoride, which is caused by the significant low activation barrier for the P−F bond formation. In addition, the unique nucleophilicity of fluoride versus hydroxide toward VX, in contrast to their relative basicity, is discussed. Although the reaction outcomes were similar, much slower reaction rates were observed experimentally for the VX-model (**1**) in comparison to VX.

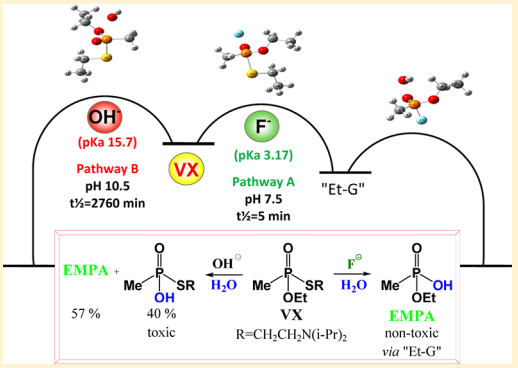

INTRODUCTION

The reactivity of the fluoride ion toward phosphyl moieties has been investigated in various disciplines of organophosphorus chemistry.[1] Kirby, Nome, and co-workers found that the nucleophilicity of fluoride toward phosphorus is greater than its basicity. In addition, the fluoride ion is nearly 3 orders of magnitude more reactive than an oxyanion of the same basicity.[1d,f] The unique strength of the P−F bond, as indicated by the enhanced thermodynamic affinity of fluoride toward the phosphoryl group, is reflected by the stability of the transition states containing partial P−F bonds.[2] Interestingly, this feature was utilized not only for synthetic purposes but also for fluoride-induced reactivation of the phosphorylated acetylcholine esterase enzyme inhibited by the nerve agent sarin (*O*-isopropyl methylphosphonofluoridate, GB).[3]

Among the chemical warfare agents (CWAs), the nerve agent VX (*O*-ethyl *S*-2-(diisopropylamino)ethyl methylphosphonothioate) is a target of prior importance in the development of decontamination methods, due to its high toxicity, environmental persistence, and low volatility.[4] In neutral to basic pH, the hydrolysis of VX leads to a mixture of products, namely ethyl methylphosphonic acid (EMPA) and *S*-2-(diisopropylamino)-ethyl methylphosphonothioic acid (desethyl-VX) resulting from the cleavage of the P−S or P−O bonds, respectively. In aqueous solutions, the relative amount of desethyl-VX was found to be affected by pH, reaching as much as 50% at pH 7−12 and ∼13% above pH 12.[4b] Desethyl-VX has similar toxicity to that of VX and is "environmentally stable" and far more persistent toward further hydrolysis.[4,5] Therefore, intense efforts are directed to the development of easy, applicable, and gentle methods for VX degradation to nontoxic products, preferably by noncorrosive aqueous media and in a catalytic manner.

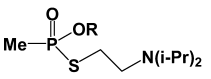

VX: R=Et
Desethyl-VX: R=H

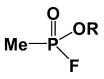

GB: R=i-Pr
Et-G: R=Et

Recently, we published our results on the detoxification of both nerve agents VX and GB under the action of water-swelled polystyrene-supported ammonium fluorides (Amberlite IRA 900 F^-).[6] It was found that during the process, VX is degraded catalytically by the heterogeneous aqueous ammonium fluoride system to the nontoxic product EMPA, via a "G-analogue" intermediate (Et-G), which is more prone to hydrolysis (Scheme 1). In the same study, we have shown that desethyl-VX is not formed and that EMPA and 2-(diisopropylamino)ethanethiol

Received: July 22, 2012
Published: October 18, 2012

Scheme 1. Catalytic VX Detoxification Process with Amberlite IRA 900 F^-

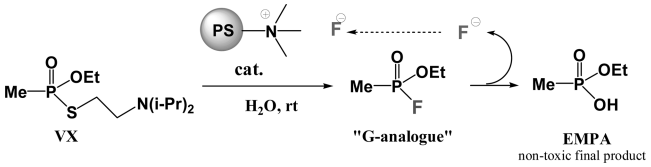

(DAT) are the sole products. In the past, we have investigated the outcome of chemical warfare agents including VX on wet KF/Al_2O_3, enriched by fluoride ions. We found that on this active support, EMPA was formed exclusively.[7] The present results, together with those obtained with Amberlite IRA 900 F^-,[6] suggest that Et-G may also be produced but immediately hydrolyzed to EMPA on wet KF/Al_2O_3.

In the present study, two questions are addressed regarding the facile degradation of VX promoted by water-solvated fluoride ions. The first is related to the mechanism of the processes, namely, to the effectiveness of the fluoride in the detoxification of VX and to the driving force for these reactions. The second question is related to the potential utility of these processes, namely, their ability to take place in homogeneous aqueous dilute solutions containing soluble fluoride ions with nearly neutral pH. Regarding the first issue, the capability to accurately elucidate reaction mechanisms involving nucleophilic transformations of P(V) compounds using ab initio and DFT methods, both in the gas phase and in solution, had been demonstrated many times during the past decade.[8,9] Therefore, we presumed that by using these methodologies and conducting a complementary mechanistic study, we shall gain a better understanding of these unique transformations (i.e., formation and subsequently hydrolysis of Et-G). Regarding the second question, from a CWAs detoxification point of view, the homogeneous nature of the decontaminant solution is critical for optimal decontamination of polluted areas. In our opinion there will be no limitation for the use of fluoride solutions in the decontamination of CWAs. Moreover, fluoride has low corrosiveness and low toxicity, and in many countries it is used as an additive in drinking water (fluoridation of water) for the prevention of tooth decay.

We disclose here our findings on the fluoride-catalyzed degradation of VX in homogeneous neutral dilute aqueous solutions. The mechanistic study relies on both experimental and computational results.

RESULTS AND DISCUSSION

Kinetic Study of VX Degradation. The degradation of VX in a series of dilute (0.066−0.33 M) aqueous fluoride salt (NaF, KF, CsF, or TBAF) solutions was examined, and the effect of the fluoride ion was determined in basic buffers, unbuffered water, and methanol. A control experiment was also conducted with KCl in unbuffered water. A fixed volume of a salt solution was placed in an NMR tube, and an appropriate amount of VX was dissolved in it. The degradation of VX was monitored under various conditions and its outcome followed mainly by ^{31}P NMR. The identity of the products was confirmed by comparison with authentic samples using ^{31}P NMR, ^{1}H NMR, and ^{19}F-NMR.[6] We were satisfied to find that even in those dilute fluoride solutions, VX was fully degraded to the final nontoxic EMPA and DAT products. Moreover, the composition of the product mixtures and the reaction profiles were similar to those found in the concentrated heterogeneous media of the water-swelled resin.[6] Namely, in the first step, a mixture of Et-G and EMPA was obtained, and at the end of the process the sole phosphorus-containing product was EMPA.

Curve-fitting of the results obtained in most of the experiments led to the following minimal kinetic model (eq 1) with calculated pseudo-first-order half-life times summarized in Table 1. To compare different reaction conditions, half-life

Table 1. Degradation Rate of VX (66 mM) in Different Media

					products (%)	
run	salt[a]	solvent	$t_{1/2}$ (VX) (min)	$t_{1/2}$ (Et-G) (min)	EMPA	desethyl-VX
1	KF	water	12	102	100	–
2	KF[a]	water	46	580	100	–
3	KF	methanol	69	158	100[b]	–
4	NaF	water	11	84	100	–
5	CsF	water	11	108	100	–
6	TBAF	water	18	149	100	–
7	TBAF[a]	water	53	nd	100	–
8	KCl	water	3465	–	68	32
9	none	water	3438	–	<50	50

[a]In all runs, 5 equiv of fluoride were used except for runs 2 and 7 where only 1 equiv was used. [b]EMMP (94%) is the main product, and EMPA (6%) is also formed.

times for both VX and Et-G degradation were calculated [$t_{1/2}$ (VX) or $t_{1/2}$ (Et-G)].

$$A \xrightarrow{k_1} B \xrightarrow{k_2} C \quad (1)$$

Figure 1 describes graphically a process in which VX (0.066M) was dissolved in an aqueous solution containing potassium

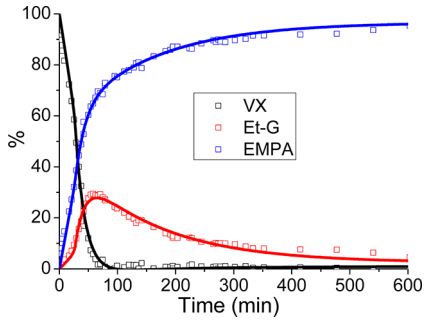

Figure 1. Curve fitting for the degradation profiles of VX (66 mM), Et-G formation and degradation, and EMPA formation in an aqueous solution containing 5 equiv of KF (run 1).

fluoride (5 equiv, Table 1, run 1). VX rapidly disappeared ($t_{1/2}$ = 12 min), but only after full hydrolysis of Et-G ($t_{1/2}$ = 102 min) does the solution become free of toxic compounds. This represents a typical reaction profile of most of the processes studied in this paper (for data concerning other experiments, see Figures S2−S14, Supporting Information). In most cases, before ca. 20% conversion was reached, the reaction was relatively slow as compared with the accelerated degradation observed later. However, even in this time period the amount of EMPA was always superior to that of Et-G (Figure 1). We hypothesized that these effects may be due to gradual changes in pH that may occur during the degradation process. This issue will be discussed later.

dx.doi.org/10.1021/jo301549z | J. Org. Chem. 2012, 77, 10042−10049

Inspection of the data presented in Table 1 emphasizes the dramatic effect of the fluoride ion on the degradation process. The degradation of VX in unbuffered water is quite slow ($t_{1/2}$ ~ 3438 min, run 9), and a significant amount of the toxic product desethyl-VX is obtained (50%).[4b,10] When only 1 equiv of KF was used, VX was degraded in less than 6 h ($t_{1/2}$ ~ 46 min) and the full hydrolysis of Et-G to EMPA took almost 2 days ($t_{1/2}$ ~ 580 min) (Table 1, run 2). Once the KF concentration was increased by 5 fold, the degradation rates of VX and of Et-G were 4 and 5 times faster, respectively. This result emphasizes the importance of the fluoride salt concentration. It also implies that VX disappears mainly through the reaction with the fluoride ion, and that the basic medium induced by KF and VX itself favors the hydrolysis of Et-G.

To learn about the role of the counterion, KF was replaced by NaF, CsF, or tetrabutylammonium fluoride (TBAF) (runs 4–6). The rates obtained were of the same order of magnitude, and no correlation could be found between the cation properties and either VX degradation or hydrolysis of Et-G (see Figure 2). These results are well correlated with the prediction

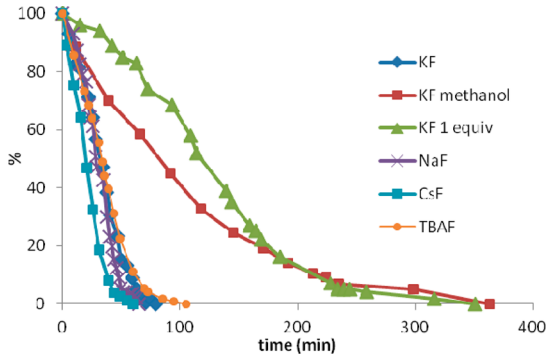

Figure 2. VX (66 mM) degradation profile in various media. The solvent is water, and 5 equiv of fluoride salt are used unless otherwise specified.

made by Churchill and Lee for the chelation of Me-VX (methyl ester VX) with Na^+ and K^+ in the gas phase.[11] They found a minor P–S bond length contraction of 0.01 Å for K^+ which renders the P–S bond scission slightly harder than that for Na^+. This would account for the small difference seen in the hydrolysis rate (runs 1 and 4). In the case of TBAF, two concentrations were examined (1 and 5 equiv, runs 6 and 7), and for the higher concentration, the degradation rate for VX was increased by a factor of 3.

To evaluate the role of the fluoride ion, a control experiment with KCl (5 equiv, run 8) was conducted. The reaction was very slow ($t_{1/2}$ ~ 2.5 d), and desethyl-VX (32%) was formed as in unbuffered water (run 9). This result emphasizes the unique role of fluoride in contrast to other nucleophiles, and particularly halides. As was previously shown with the fluoride solid-supports (KF-Al_2O_3 and Amberlite IRA 900 F^-), the main advantage of using fluorides, in contrast to basic media, is to prevent the desethyl-VX formation and to significantly reduce the corrosivity.[6,7] The hydrolysis of VX by hydroxide solutions (KOH or NaOH) was intensively explored and well documented.[4] These reactions were found to be strongly dependent on both the pH and the temperature and always yielded a mixture of EMPA and desethyl-VX. The present study shows that in basic buffers the presence of fluoride not only improves the degradation rate of VX but also prevents the formation of desethyl-VX.

To elucidate whether the reaction profile depends on solvation properties of the species involved in the process, a similar experiment was performed in methanol as an organic protic polar solvent. A similar degradation profile was observed in methanol, but the degradation rate of VX was 5-fold slower ($t_{1/2}$ ~ 69 min, run 3). In addition, Et-G, which did not accumulate over 6%, was converted to ethyl methyl methylphosphonate (EMMP) at a rate similar to that found in water for the generation of EMPA. These results imply that Et-G undergoes very fast methanolysis and/or that direct methanolysis of VX is preferred over the formation of Et-G. Our calculations unambiguously show that both hypotheses are valid (vide infra).

pH Effect. Another parameter which may influence the reaction profile is the pH. The initial pH of the fluoride solution was ~8.0. With the addition of the amino basic compound, VX, the pH instantaneously increased to 10.7. A continuous measurement of the pH during the degradation of VX (5 equiv of KF in water, run 1) showed that the pH decreased from 10.7 to 7.0 toward the end of the reaction (see Figure 3). This

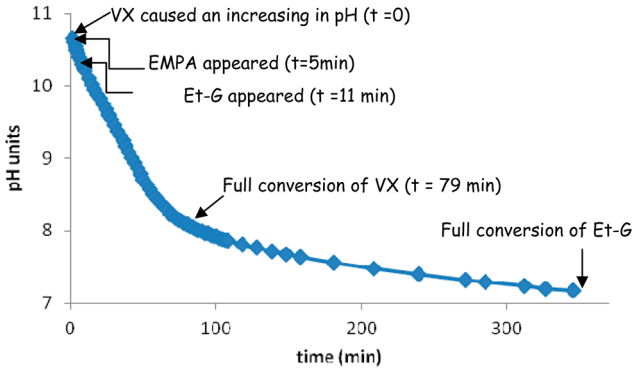

Figure 3. pH change during the degradation of VX in the presence of KF (run 1).

decrease was fast at the beginning of the process and became slower after full disappearance of VX (pH 8.11). Because Et-G began to accumulate as the pH decreased, we hypothesized that if the pH is maintained at its original value (~10.5), any Et-G formed will be immediately hydrolyzed to EMPA. Accordingly, an experiment in which KF was dissolved in a carbonate–bicarbonate buffer solution (0.1 M, pH 10.5) was performed. As expected, no Et-G could be detected during the rapid degradation of VX ($t_{1/2}$ = 32 min, run 10), desethyl-VX was not formed, and EMPA was the only product. We concluded that at basic pH, the degradation of Et-G is favored in such a way that its hydrolysis is faster than its formation. Interestingly, in a buffered aqueous solution (pH 10.5) lacking fluoride, the degradation rate of VX was very slow ($t_{1/2}$ ~ 2760 min, run 14) and desethyl-VX was formed (40%) together with EMPA (50%) and traces of methyl phosphonothioate ethyl ester (6%). Other buffered solutions with pHs of 7.45, 8.84, and 9.65 were also examined. As expected, while the medium becomes less basic, the VX degradation rate increases, Et-G hydrolysis becomes slower, and so more Et-G accumulates (see Table 2). At pH 7.45, we observed for the first time a situation in which the amount of Et-G was superior to that of EMPA until VX almost disappeared (see Figure 4). This profile entirely fits the above-mentioned minimal kinetic model in eq 1, even at the beginning of the reaction.

In light of these results, it is clear that the reactions that occur during the degradation process of VX begin with a very fast

dx.doi.org/10.1021/jo301549z | J. Org. Chem. 2012, 77, 10042–10049

Table 2. Degradation Rate of VX (66 mM) at Different pH with KF (5 equiv) or without Fluoride

run	salt	media	$t_{1/2}$ (VX) (min)	$t_{1/2}$ (Et-G) (min)	EMPA (%)	desethyl-VX (%)
10	KF	buffer[a] 10.50	32	–	100	–
11	KF	buffer[a] 9.65	17	17	100	–
12	KF	buffer[b] 8.84	20	20	100[c]	–
13	KF	buffer[b] 7.45	5	44	100[c]	–
14	–	buffer[a] 10.50	2760	–	54	40

[a]Carbonate–bicarbonate buffer (0.1 M). [b]Tris buffer (0.1 M). [c]Part of EMPA is esterified by the triol present in Tris buffer.

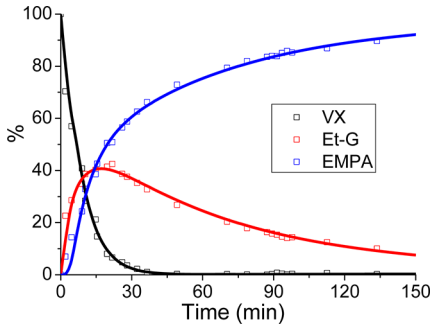

Figure 4. VX (66 mM) degradation profile in a pH 7.45 buffer solution containing 5 equiv of KF (run 13).

nucleophilic substitution of the aminoethylthiolate group by fluoride ion (k_1) followed by hydrolysis (k_2). The rates of both steps depend on the pH. In basic media (pH > 10), in the presence of fluoride, the hydrolysis is so fast that Et-G could not be detected ($k_1 \ll k_2$). As the pH is decreased to almost neutral, the hydrolysis rate is not sufficient to immediately decompose Et-G once it is formed ($k_1 > k_2$). Between basic and neutral pH, the hydrolysis is fast enough so that the amount of EMPA is superior to that of Et-G, but it is low enough to allow the accumulation of Et-G. In nonbuffered solutions, the pH decreases as EMPA is formed. The beginning of the process has a profile similar to that found for buffer 9.65 (run 11), but later the reaction is slowed down by the decrease in pH.

Quantum Mechanical Study. Quantum mechanical methods were previously shown to yield accurate results in theoretical studies of analogous nucleophilic attacks on various phosphates[8] and phosphonates[9] including CWAs.[12] As a model for VX we used *O*,*S*-diethyl methylphosphonothioate (**1**) and studied the reactions' pathways which may evolve from nucleophilic attacks by fluoride, hydroxide, or methoxide anions. Similar analogy was previously used successfully by Patterson and co-workers[13] who produced results which were in excellent agreement with the available experimental data.[14] It should also be noted that, theoretically, attack at the ester/thio ester carbon is also possible, as shown to occur for several phosphate triesters in the gas phase.[8c,g,h,15] Nevertheless, we[9h,16] and others[9e,13,17] showed that in solution only attack at the phosphorus takes place as expected from hard nucleophiles.[18] Therefore, we neglected processes which comprise an attack of the nucleophiles on atoms other than P.

To carefully evaluate all plausible reaction pathways which may evolve from an initial attack of either fluoride, hydroxide, or methoxide nucleophile at the P center of the model compound (Scheme 2), all starting materials, transition states, and products were fully optimized in the gas phase and in solution (water and methanol), and their thermodynamic data

Scheme 2. Calculated Pathways for the Reaction of *O*,*S*-Diethyl Methylphosphonothioate (1)

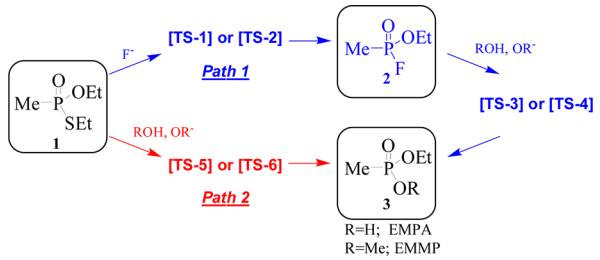

were obtained from frequency calculations using B3LYP/6-311G+(d,p) level of theory (Table S21, Supporting Information). To check the validity of this DFT method, single-point energies were also calculated at the MP2/6-31G+(d) level (Table 3). Some relatively large discrepancies were found

Table 3. Relative Free Energies[a] (kcal mol^{-1}) for the Reactions Shown in Scheme 2 and Transition States

	relative free energies MP2/6-31G+(d)//B3LYP/6-311G+(d,p)		
reactions and transition states	gas phase	water	methanol
TS1	−10.7	16.8	17.3
TS2	−12.0	17.9	17.2
TS3(H)	−29.9	9.9	
TS3(Me)	−37.5		1.7
TS4(H)	−29.8	10.6	
TS4(Me)	−32.9		3.6
TS5(H)	−6.8	19.1	
TS5(Me)	−10.7		15.3
TS6(H)	−12.5	16.9	
TS6(Me)	−16.2		13.3
PR1 (Et-G + EtS$^-$)	−22.1	−2.1	−7.9
PR2 (EMPA + EtS$^-$)	−40.7	−24.0	
PR3 (EMMP + EtS$^-$)	−40.6		−33.1

[a]Energies are relative to starting materials which are defined as zero.

between the two methods. The most pronounced difference was found for the energy values of the species that evolved from fluoride attack in water. Moreover, recalculating these species at the B3LYP level of theory using SMD as the solvation model,[19] we obtained results much closer to those obtained at MP2 level with IEF-PCM solvation model. Therefore, we use in our discussion the more reliable MP2 results.

In principle, two modes of attack should be considered: one is opposite to the thioester group or to the fluorine in Et-G (**2**), and the second is opposite to the ester group (see odd and even numbers for TSs, respectively, Figure 5). The preference between the two modes should be dictated by the relative stability of the trigonal bipyramidal transition states formed, namely, according to the apicophilicity of the ligands around the phosphorus center.[20] Two possible pathways (paths 1 and 2, Scheme 2) for the formation of the final products were studied. Path 1 is a two-step reaction in which there is a nucleophilic attack by F$^-$ anion via either **TS1** or **TS2** on **1** to initially form Et-G (**2**). The final product **3** (EMPA or EMMP) is obtained via **TS3** or **TS4** by hydrolysis/methanolysis using the corresponding nucleophile. Path 2, on the other hand, would not involve the formation of Et-G but rather the direct hydrolysis/methanolysis of **1**, via **TS5** or **TS6**. Calculating the

dx.doi.org/10.1021/jo301549z | J. Org. Chem. 2012, 77, 10042–10049

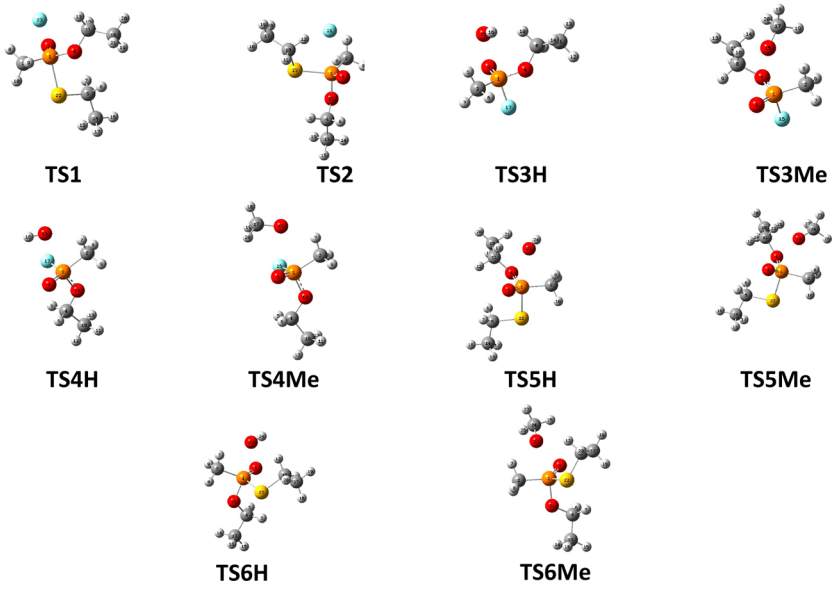

Figure 5. Three-dimensional structures of the calculated transition states. (Orange = phosphorus, red = oxygen, gray = carbon, yellow = sulfur, cyan = fluorine).

kinetics of path 2 in comparison to those of path 1 would shed more light on our experimental results. In studying the structure of all the possible transition states (Figure 5) it is clear that **TS1**, **TS3**, and **TS5**, in which the corresponding P−S and P−F bonds are apical, have the correct geometry needed for the formation of products **2** or **3** following the cleavage of the appropriate bonds. However, even if the favored transition states are **TS2**, **TS4**, and **TS6**, the products **2** and **3** should be obtained after a pseudorotation process of an initial trigonal bipyramid intermediate, which is formed during the nucleophilic attack. Such pseudorotations are well-known processes and are usually low in energy demand,[9h,21] although in the case of VX and its model, Patterson found them to be substantial and energetically costly.[13] Nevertheless, by keeping in mind that experimentally we did not detect by NMR any trace of desethyl-VX (P−O cleavage), it is clear that only two modes of attack involving P−S cleavage are relevant. The first should comprise an attack opposite to the thiolate ligand (**TS1** or **TS5**) followed by cleavage of the P−S bond. The second would involve pseudorotation of the intermediate which evolves from attack opposite to the OEt ligand (**TS2** or **TS6**), to form a new intermediate in which the SEt and the CH_3 fragments are both apical. The latter intermediate would next undergo P−S bond scission to give **2** or **3**. In any case, Patterson established[13c] that the initial attack is the rate-determining step. Therefore, on the basis of his results, we feel confident to neglect any other intermediates formed.

Calculated Reaction in Water. From examining the four possible transition states (**TS1**, **TS2**, **TS5**, and **TS6**) which evolve from a nucleophilic attack on **1** (Table 3 and Figure 6), it is clear that the nucleophilicity of F^- and OH^- is similar with a slight preference for the fluoride. This is unexpected if one considers their relative basicity, as was also previously observed by others.[1] The calculated free energy for the formation of these transition states are 16.8, 17.9, 19.1, and 16.9 kcal/mol, respectively. It should also be noted that the barriers for the OH^- attack are in good agreement with previously reported calculations by Patterson and co-workers.[12b,c] Thermodynamically, we found that the formation of **2** from **1** in water is

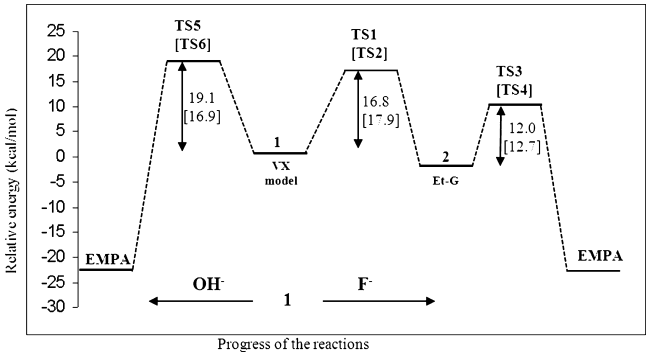

Figure 6. Reaction profiles for the degradation of VX-analogue **1** in water.

slightly exothermic by 2.1 kcal/mol. Once **2** is formed, it would undergo an attack by OH^-, via **TS3(H)** or **TS4(H)**. We calculated the activation free energies of these transition states in water to be 12.0 and 12.7 kcal/mol, respectively, again in good agreement with previously reported values for sarin.[13b] Notably, although the energy difference between these two transition states was calculated to be only 0.7 kcal/mol, both should eventually lead to the formation of **3**. The analysis leads to the conclusion that in path 1, the attack of fluoride is the rate-determining step. All the above explain very well the experimental fact that Et-G is initially accumulating in substantial amounts (for example, see run 1 and Figure 1) unless the pH is basic (see run 10 and Figure S9, Supporting Information). We cannot exclude the possibility of some equilibrium between **1** and **2** at room temperature and low pH, although a substantial difference in activation barriers is expected, as **PR1** is 2.1 kcal/mol lower in energy than the starting materials (Table 3).

Calculated Reaction in Methanol. Comparing the calculated values in water with those in methanol, a somewhat different picture emerges (Figure 7). The calculated activation energies for the formation of Et-G (path 1, **TS1** or **TS2**) and the direct methanolysis of **1** [path 2, **TS5(Me)** or **TS6(Me)**] are 17.3, 17.2, 15.3, and 13.3 kcal/mol, respectively. Namely, direct methanolysis by methoxide, either via attack opposite to

dx.doi.org/10.1021/jo301549z | J. Org. Chem. 2012, 77, 10042−10049

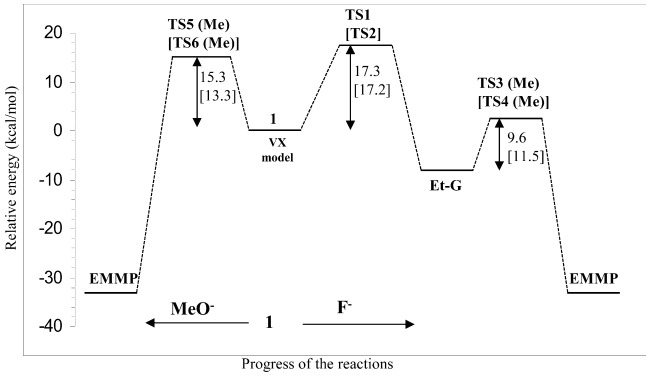

Figure 7. Reaction profiles for the degradation of VX-analogue **1** in methanol.

the thiolate or via attack opposite to the OEt followed by a fast pseudorotation, is preferred by at least 2 kcal/mol over an attack by F^- (providing of course that the pH is basic). Moreover, inspection of path 1 reveals that the formation of Et-G is the rate-determining step, as the calculated free energy of activation for the formation of **TS3(Me)** and **TS4(Me)** are 9.6 and 11.5 kcal/mol, respectively. The barrier for the second step is significantly much lower in methanol than in water. According to our calculations, both mechanisms (direct methanolysis versus formation of Et-G followed by its methanolysis) may coexist in methanol, albeit to a lesser extent than in the parallel process in alkaline water. Thermodynamically, we found that the formation of **2** from **1** in methanol is more exothermic by 7.9 kcal/mol (in contrast with 2.1 kcal/mol found in water), and the entire process is exothermic by 33.1 kcal/mol (compared to 24.0 kcal/mol found in water). These computations support the observation made in methanol (run 3) in which the level of Et-G was very low all along the process because methanolysis of VX was slightly preferred to fluoride attack, and in parallel, methanolysis of Et-G was a fast process compared to its formation (Figure S3, Supporting Information). Moreover, it explains the kinetic results in water compared with methanol (runs 1 and 3 and Figure 2).

Kinetics of VX-Model 1 Degradation. The calculated energies in this work fit well with the above-mentioned experimental results both in terms of kinetics and products identity. In their comparative theoretical mechanistic study on the hydrolysis of VX-model **1**[13b] versus VX,[13c] Patterson and co-workers concluded that "the same mechanism is elucidated by either the model or VX and it is apparent that nucleophilic chemistry at the phosphorus atom in VX can be accurately predicted using small model systems". However, they also reported some differences between these two phosphonothioate analogues. Among them, the most important is that the bulky aminothiolate moiety in VX may pose a significant steric effect on the stability of the trigonal bipyramide intermediate. To clarify this point in our fluoride/methylphosphonothioate system from both kinetics and products identity points of view, we explored the reactions of VX-model **1** with fluoride under the same conditions mentioned above. We found that this less hindered amine-free methylphosphonothioate compound reacts with fluoride ions in a similar manner, in which Et-G is formed as an intermediate that eventually hydrolyzed to EMPA (Table 4). The increased reactivity of fluoride versus hydroxide seems yet again, unambiguous, when inspecting the reactions data of **1** with and without fluoride in basic buffer (runs 16 and 17). However, we were quite surprised to find that the reaction of

Table 4. Degradation Rate of 1 (66 mM) with KF (5 equiv) or without Fluoride in Aqueous Solutions

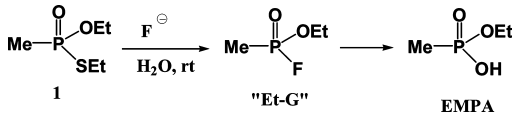

run	salt	media	$t_{1/2}$ (**1**) (min)	$t_{1/2}$ (Et-G) (min)	EMPA (%)	desethyl-**1** (%)
15	KF	water	861	571	100	–
16	KF	buffer[a] 10.50	876	–	100	–
17	–	buffer[a] 10.50	$>2.4 \times 10^4$	–	35[b]	9[b]

[a]Carbonate–bicarbonate buffer. [b]After 333 h reaction.

1 is much slower than that of VX itself (compare run 15 versus run 1, or run 16 versus run 10). We believe that the steric effect mentioned above cannot explain by itself this remarkable difference. This effect has to be thoroughly studied in a more general perspective.

CONCLUSION

We have shown by both theoretical and experimental studies that the fluoride ion is very reactive toward the phosphorus atom in compounds such as VX, especially in water. Degradation experiments in dilute aqueous fluoride solutions show that VX, an extremely toxic and environmentally stable compound, rapidly converts to the nontoxic product EMPA via the intermediate Et-G (5 equiv of fluoride; $t_{1/2}$[VX] 12 min; $t_{1/2}$[Et-G] 102 min). The toxic side product desethyl-VX, which forms in substantial quantities during the degradation of VX in unbuffered water, is completely avoided in this aqueous fluoride homogeneous environment. In methanol, the reaction rates are slower for the degradation of VX and Et-G by a factor of 6 and 1.5, respectively. Typically the hydrolysis of Et-G is the rate-determining step, and it strongly depends on the pH evolving during the reaction. When the pH is maintained at its initial level (10.5) by a buffer, the hydrolysis of Et-G is so fast that no Et-G can be detected. Our quantum mechanical calculations on a VX-model clearly demonstrate the unique role of the fluoride ion in this facile degradation process. The similar reactivity of fluoride versus hydroxide is reflected by the significant low transition state energy in the case of fluoride which was unexpected considering their relative basicity. We are currently extending our study to other general organophosphorus compounds such as phosphites, phosphonates, and phosphates, and more particularly, the reasons for the remarkable difference in reaction rates of VX versus VX-model **1** with fluoride are under investigation.

EXPERIMENTAL SECTION

Materials. The organophosphorus compounds were of high purity (>99%) and did not contain any of the hydrolysis products. VX was obtained locally at IIBR using standard methods.[22] The different fluoride salts were purchased from Sigma-Aldrich.

NMR. ^{31}P and ^{19}F MAS NMR spectra were obtained at 202 and 471 MHz, respectively, on a 11.7 T (500 MHz) spectrometer. Chemical shifts for ^{31}P and ^{19}F were referenced to external trimethyl phosphate (TMP) and $CFCl_3$, respectively, as 0 ppm. For ^{31}P spectra, the pulse delay was 2 s. The frequency offset was set between the signals of VX and EMPA. For comparison purposes, spectra were recorded under identical conditions.

Curve Fitting. The kinetic models for the degradation reactions were solved by orthonormalization of the species population's vectors according to the Gram–Schmidt process. The time-dependent population vectors were extracted from the NMR experiments by

dx.doi.org/10.1021/jo301549z | J. Org. Chem. 2012, 77, 10042–10049

mathematical integration over a best fitting to Gaussian functions. The fit was preceded by the removal of the experimental noise using singular value decompostion (SVD). The Gaussian function was determined because of better convergence to ~0.505 Hz spectral resolution,[23] this in comparison to Lorentz and Voigt functions which give overestimation. The extracted populations were normalized to one at each time sequence and then were fed into the mathematical model.[24,25] In all cases, the finite instrument response determined by the interferometry time is included in the fitting procedure by convolving the model matrix by Gaussian width of fwhm ~2 min.

Description of the Computational Methods. Optimized geometries and harmonic frequencies for all the reported species (starting materials, transition states, intermediates, and products) were obtained by density functional calculations using the B3LYP hybrid functional and 6-311+G(d,p) basis set (corrected for unscaled ZPVE).[26a] Gas-phase optimized structures were used as input for the calculations in solution which were reoptimized at the same level of theory with the integral equation formalism polarized continuum solvation model (IEF-PCM).[27] Energies from these calculations were converted to thermodynamic data based on the frequency calculations. More accurate electronic energies were obtained via single-point calculations at the MP2/6-31G+(d) level of theory. These calculations were performed on the converged geometries in the gas phase and in solution, respectively.[26] Thermal correction to Gibbs free energy was obtained from frequency calculations in the gas phase and in solution, respectively. All energies in solution (at MP2 level) include both electrostatic and nonelectrostatic corrections.[26b] All transition states were verified by calculating the intrinsic reaction coordinates (IRC) and/or by examining the imaginary frequency's normal mode.[28]

Sample Preparation. *Caution: These experiments should only be performed by trained personnel using applicable safety procedures.* Salt solutions were prepared by dissolving the appropriate amounts of salt (KF, NaF, CsF, TBAF, KCl) or KOH in water or buffered aqueous solution or methanol. Two kinds of solutions were prepared containing 1 or 5 equiv of salts per OP equivalent. An amount of 1 or 5.3 μL (13.2 mM or 66 mM) of the OP compound (VX or VX-model **1**) was applied via a syringe to a Teflon NMR tube containing 300 μL of the salt solution. The tube was sealed with a Teflon cap and inserted in a glass NMR tube. ^{31}P and ^{19}F MAS NMR spectra were measured periodically to determine the amount of remaining starting material and identify degradation products. The buffered solutions (0.1 M each) were prepared by standard procedures,[29] carbonate–bicarbonate buffer for pH 10.5 and 9.65 and Tris buffer for pH 8.64 and 7.45. Tris buffer contains 3-amino-3-(2-hydroxyethyl)pentane-1,5-diol, which reacts with EMPA to give the corresponding ester detected by ^{31}P NMR at δ 32 ppm. It was assumed that it does not dramatically affect the outcome of the processes.

■ ASSOCIATED CONTENT

Supporting Information

Kinetic data of the reactions, NMR spectra, absolute energies, and number of imaginary frequencies and optimized geometries for all calculated species performed in different solutions. This material is available free of charge via the Internet at http://pubs.acs.org.

■ AUTHOR INFORMATION

Corresponding Author

*E-mail: yossiz@iibr.gov.il; nissan.ashkenazi@iibr.gov.il.

Author Contributions

§These authors contributed equally.

Notes

The authors declare no competing financial interest.

■ ACKNOWLEDGMENTS

This work was internally funded by the Israeli Prime Minister's office.

■ REFERENCES

(1) Selected articles: (a) Kirby, A. J.; Lima, M. F.; da Silva, D.; Roussev, C. D.; Nome, F. *J. Am. Chem. Soc.* **2006**, *128*, 16944–16952. (b) Kirby, A. J.; Lima, M. F.; da Silva, D.; Nome, F. *J. Am. Chem. Soc.* **2004**, *126*, 1350–1351. (c) Admiraal, S. J.; Herschlag, D. *J. Am. Chem. Soc.* **1999**, *121*, 5837–5845. (d) Herschlag, D.; Jencks, P. *J. Am. Chem. Soc.* **1990**, *112*, 1951–1956. (e) Kirby, A. J.; Younas, M. *J. Chem. Soc. (B)* **1970**, 1165–1172. (f) Khan, S. A.; Kirby, A. J. *J. Chem. Soc. B* **1970**, 1172–1182.

(2) (a) Fey, N.; Garland, M.; Hopewell, J. P.; McMullin, C. L.; Mastroianni, S.; Orpen, A. G.; Pringle, P. G. *Angew. Chem., Int. Ed.* **2012**, *51*, 118–122. (b) Grant, D. J.; Matus, M. H.; Switzer, J. R.; Dixon, D. A.; Francisco, J. S.; Christe, K. O. *J. Phys. Chem. A* **2008**, *112*, 3145–3156. (c) Kirby, A. J.; Warren, S. G. In *The Organic Chemistry of Phosphorus*; Elsevier Publishing Co.: London, 1966; p 5.

(3) Van der Schans, M. J.; Polhuijs, M.; Van Dijk, C.; Degenhardt, C. E. A. M.; Pleijsier, K.; Langenberg, J. P.; Benschop, H. P. *Arch. Toxicol.* **2004**, *78*, 508–524.

(4) Selected articles: (a) Kim, K.; Tsay, O. G.; Atwood, D. A.; Churchill, D. G. *Chem. Rev.* **2011**, *111*, 5345–5403. (b) Groenewold, G. S. *Main Group Chem.* **2010**, *9*, 221–244. (c) Brevett, C. A. S.; Sumpter, K. B. *Main Group Chem.* **2010**, *9*, 205–219. (d) Vayron, P.; Renard, P.-Y.; Taran, F.; Creminon, C.; Frobert, Y.; Grassi, J.; Mioskowski, C. *Proc. Natl. Acad. Sci. U.S.A.* **2000**, *97*, 7058–7063. (e) Yang, Y.-C. *Acc. Chem. Res.* **1999**, *32*, 109–115.

(5) Cragan, J. A.; Ward, M. C.; Mueller, C. B. *J. Hazard. Mater.* **2009**, *170*, 72–78.

(6) Marciano, D.; Goldvaser, M.; Columbus, I.; Zafrani, Y. *J. Org. Chem.* **2011**, *76*, 8549–8553.

(7) (a) Zafrani, Y.; Yehezkel, L.; Goldvaser, M.; Marciano, D.; Waysbort, D.; Gershonov, E.; Columbus, I. *Org. Biomol. Chem.* **2011**, *9*, 8445–8451. (b) Gershonov, E.; Columbus, I.; Zafrani, Y. *J. Org. Chem.* **2009**, *74*, 329–338.

(8) Examples for phosphates: (a) Dejaegere, A.; Karplus, M. *J. Am. Chem. Soc.* **1993**, *115*, 5316–5317. (b) Dejaegere, A.; Liang, X.; Karplus, M. *J. Chem. Soc., Faraday Trans.* **1994**, *90*, 1763–1770. (c) Chang, N.-Y.; Lim, C. *J. Phys. Chem. A* **1997**, *101*, 8706–8715. (d) Chang, N.-Y.; Lim, C. *J. Am. Chem. Soc.* **1998**, *120*, 2156–2167. (e) Florian, J.; Warshel, A. *J. Phys. Chem. B.* **1998**, *102*, 719–734. (f) Hu, C.-H.; Brinck, T. *J. Phys. Chem. A* **1999**, *103*, 5379–5386. (g) Lopez, X.; Dejaegere, A.; Karplus, M. *J. Am. Chem. Soc.* **2001**, *123*, 11755–11763. (h) Menegon, G.; Loos, M.; Chaimovich, H. *J. Phys. Chem. A* **2002**, *106*, 9078–9084. (i) Arantes, G. M.; Chaimovich, H. *J. Phys. Chem. A* **2005**, *109*, 5625–5635. (j) López, C. S.; Faza, O. N.; de Lera, A. R.; York, D. M. *Chem.—Eur. J.* **2005**, *11*, 2081–2093. (k) Iché-Tarrat, N.; Barthelat, J.-C.; Rinaldi, D.; Vigroux, A. *J. Phys. Chem. B* **2005**, *109*, 22570–22580. (l) Lopez, X.; Dejaegere, A.; Leclerc, F.; York, D. M.; Karplus, M. *J. Phys. Chem. B* **2006**, *110*, 11525–11539.

(9) Examples for phosphonates: (a) Thatcher, G. R. J.; Campbell, A. S. *J. Org. Chem.* **1993**, *58*, 2272–2281. (b) Zheng, F.; Zhan, C.-G.; Ornstein, R. L. *J. Chem. Soc,. Perkin Trans. 2* **2001**, 2355–2363. (c) Bell, A. J.; Citra, A.; Dyke, J. M.; Ferrante, F.; Gagliardi, L.; Watts, P. *Phys. Chem. Chem. Phys.* **2004**, *6*, 1213–1218. (d) Barbosa, A. C. P.; Borges, I., Jr.; Lin, W. O. *J. Mol. Struct. (THEOCHEM)* **2004**, *712*, 187–193. (e) Doskocz, M.; Roszak, S.; Majumdar, D.; Doskocz, J.; Gancarz, R.; Leszczynski, J. *J. Phys. Chem. A* **2008**, *112*, 2077–2081. (f) McAnoy, A. M.; Paine, M. R. L.; Blanksby, S. J. *Org. Biomol. Chem.* **2008**, *6*, 2316–2326. (g) Mandal, D.; Mondal, B.; Das, A. K. *J. Phys. Chem. A* **2010**, *114*, 10717–10725. (h) Ashkenazi, N.; Segall, Y.; Chen, R.; Sod-Moriah, G.; Fattal, E. *J. Org. Chem.* **2010**, *75*, 1917–1926.

(10) Szafraniec, L. J.; Szafraniec, L. L.; Beaudry, W. T.; Ward, J. R. ADA-250773; U.S. Army Chemical Research, Development and Engineering Center, Aberdeen Proving Ground: Aberdeen, MD, 1990.

(11) Bandyopadhyay, I.; Kim, M. J.; Lee, Y. S.; Churchill, D. G. *J. Phys. Chem. A* **2006**, *110*, 3655–3661.

(12) (a) Zheng, F.; Zhan, C.-G.; Ornstein, R. L. *J. Chem. Soc., Perkin Trans. 2* **2001**, 2355–2363. (b) Menke, J. L.; Patterson, E. V. *J. Mol.*

Struct. (THEOCHEM) **2007**, *811*, 281. (c) McAnoy, A. M.; Williams, J.; Paine, M. R.; Rogers, M. L.; Blanksby, S. J. *J. Org. Chem.* **2009**, *74*, 9319−9327. (d) Bera, N. C.; Maeda, S.; Morokuma, K.; Viggiano, A. A. *J. Phys. Chem. A* **2010**, *114*, 13189−13197. (e) Midey, A. J.; Miller, T. M.; Viggiano, A. A. *Int. J. Mass Spectrom.* **2012**, *315*, 1−7.

(13) (a) Patterson, E. V.; Cramer, C. J. *J. Phys. Org. Chem.* **1998**, *11*, 232−240. (b) Šečkutė, J.; Menke, J. L.; Emnett, R. J.; Patterson, E. V.; Cramer, C. J. *J. Org. Chem.* **2005**, *70*, 8649−8660. (c) Daniel, K. A.; Kopff, L. A.; Patterson, E. V. J. *Phys. Org. Chem.* **2008**, *21*, 321−328.

(14) Yang, Y.-C. *Acc. Chem. Res.* **1999**, *32*, 109−115.

(15) (a) Hodges, R. V.; Sullivan, S. A.; Beauchamp, J. L. *J. Am. Chem. Soc.* **1980**, *102*, 935−938. (b) Lum, R. C.; Grabowski, J. J. *J. Am. Chem. Soc.* **1992**, *114*, 8619−8627.

(16) Ashkenazi, N.; Zade, S. S.; Segall, Y.; Karton, Y.; Bendikov, M. *Chem. Commun.* **2005**, 5879−5881.

(17) (a) Haake, P. C.; Westheimer, F. H. *J. Am. Chem. Soc.* **1961**, *83*, 1102−1109. (b) Kluger, R.; Covitz, F.; Dennis, E.; Williams, L. W.; Westheimer, F. H. *J. Am. Chem. Soc.* **1969**, *91*, 6066−6072. (c) Kluger, R.; Thatcher, G. R. *J. Am. Chem. Soc.* **1985**, *107*, 6006−6011. (d) Kluger, R.; Thatcher, G. R. *J. Org. Chem.* **1986**, *51*, 207−212.

(18) Bunton, C. A. *Acc. Chem. Res.* **1970**, *3*, 257−265.

(19) Cramer, C. J.; Truhlar, D. G. *Acc. Chem. Res.* **2008**, *41*, 760−768.

(20) (a) Trippett, S. *Pure Appl. Chem.* **1974**, *40*, 595−604. (b) Trippett, S. *Phosphorus, Sulfur Relat. Elem.* **1976**, *1*, 89−98.

(21) (a) Westheimer, F. H. *Acc. Chem. Res.* **1968**, *1*, 70−78. (b) Gillespie, P.; Hoffman, P.; Klusacek, H.; Marquarding, D.; Pfohl, S.; Ramirez, F.; Tsolis, E. A.; Ugi, I. *Angew. Chem., Int. Ed.* **1971**, *10*, 687−715. (c) Gillespie, P.; Ramirez, F.; Ugi, I.; Marquarding, D. *Angew. Chem., Int. Ed.* **1973**, *12*, 91−119. (d) Hoffman, R.; Howell, J. M.; Muetterties, E. L. *J. Am. Chem. Soc.* **1972**, *94*, 3047−3058.

(22) Black, R. M.; Harrison, J. M. The chemistry of organophosphorus chemical warfare agents. In *The chemistry of organophosphorus compounds*; Hartley, F. R., Ed.; John Wiley and Sons Ltd.: Chichester, England, 1996; Vol *4*, pp 783−798.

(23) The procedure effect is depicted in Figure S1 in the Supporting Information.

(24) Ernsting, N. P.; Kovalenko, S. A.; Senyushkina, T.; Saam, J.; Farztdinov, V. *J. Phys. Chem. A* **2001**, *105*, 3443−3453.

(25) Shoshana, O.; Pe'rez Lustres, J. L.; Ernsting, N. P.; Ruhman, S. *Phys. Chem. Chem. Phys.* **2006**, *8*, 2599−2609.

(26) (a) *Gaussian 03, Revision D.01*; Gaussian, Inc., Wallingford, CT, 2004. (b) *Gaussian 09, Revision B.01*; Gaussian, Inc., Wallingford, CT, 2010. For full citation, see Supporting Information.

(27) (a) Cossi, M.; Barone, V.; Cammi, R.; Tomasi, J. *J. Chem. Phys. Lett.* **1996**, *255*, 327−335 and references cited therein. (b) Cances, E.; Mennucci, B.; Tomasi, J. *J. Chem. Phys.* **1997**, *107*, 3032−3041.

(28) Gonzalez, C.; Schlegel, H. B. *J. Chem. Phys.* **1989**, *90*, 2154−2161.

(29) Mohan, C. *Buffers - A guide for the preparation and use of buffers in biological systems*; CALBIOCHEM, EMD Biosciences, Inc., an Affiliate of Merck KGaA: Darmstadt, Germany, 2003.